Relating Fundamental Chemistry and Smart Materials with DFT Calculations

Yashar Yourdshahyan, Ilya Grinberg, Na Sai, Valentino R. Cooper, Sara E. Mason, and Andrew M. Rappe
Department of Chemistry and Laboratory for Research on the Structure of Matter, University of Pennsylvania, Philadelphia, PA
rappe@sas.upenn.edu

Russell P. Kauffman
Department of Physics, Muhlenberg College, Allentown, PA
kauffman@hal.muhlberg.edu

Abstract

We present first-principles investigations of the properties of piezoelectric oxides and metal surfaces. Our oxide work elucidates important fundamental relationships between local atomic structure and macroscopic properties of piezoelectrics. We develop a new semi-empirical model to study large supercells of disordered complex oxides. We also present our computational materials design studies of proposed new perovskites. In particular we demonstrate for the first time the off-centering behavior of silver ions, which may lead to environmentally friendly silver-based piezoelectrics. Examining the chemical properties of metal surfaces, we present our studies in vacancy formation, the effects of strain on the adsorptive properties of metal surfaces and self assembled monolayers. We find that vacancy formation leads to electronic spillout and a strengthening of the bonds between the neighboring atoms accompanied by an inward relaxation. Our calculations show that the effect of strain on the chemisorption is sensitive to changes in coverage, metal identity and surface plane. In our studies on self assembled monolayers, we examine the complex adsorption process and the potential energy surfaces for adsorption of thiols on noble metal surfaces. We also show that formation of ordered thiol structures is favorable on Al(111) surface, indicating a possible use of self-assembled monolayers as a anti-corrosion protective coating.

1. Introduction

Materials that can sense the changes in their environment and respond to it are increasingly sought in high-technology applications. Such smart materials are particularly important in dealing with the challenging operating conditions and requirements of military applications. Most smart materials are complex systems with some degree of disorder which makes them challenging to study experimentally and theoretically. However, as it is their complexity which give them their favorable properties, studies of simple model systems often cannot be used to explain the behavior of current materials and predict favorable compositions for new materials.

Recently, a combination of methodological improvements and rise in computer speed has made first-principles calculations a viable tool for understanding these complex systems. In particular, the density functional theory (DFT) approach[1,2] offers a combination of accuracy and computational speed that can reveal the microscopic structure and interactions of complex systems. Consequently, first-principles based methods can now be used to perform computational materials design, reducing the costly experimental trial and error process, which until now has been the mainstay of new materials development.

In this paper, we will report on progress achieved in our computational studies of complex piezoelectric ceramics and chemical processes on metal surfaces, two areas with great military and civilian applications.

Complex ferroelectric oxides have a wide range of structural, electrical and mechanical properties, making them well suited for many technological applications, such as ultrasound machines, cell phones, and computer memory devices. Smart materials with high piezoelectric response are of particular interest as they can be employed as sensors in SONAR devices. When such a material is deformed by underwater sound vibrations, it generates an electric field which can then be interpreted by a computer to gain information, such as depth and

Proceedings of the 2003 User Group Conference (DoD_UGC'03)
0-7695-1953-9/03 $17.00 © 2003 IEEE

distance. This information is vital for the defense and operation of naval submarines and vessels.

Processes that occur at the interface between a gas and a metal surface play a key role in sensors, catalysis and corrosion. Despite the widespread use of such processes, they are often poorly understood. A fundamental under-standing of molecular adsorption on active metal surfaces is a crucial first step in understanding industrial catalysis and the commonplace but complex corrosion process. In particular, local atomic structure and its dependence on strain, defects such as vacancies, and the arrangement of the adsorbate molecules on the surface, needs to be known. The local structural information can then enable an intelligent design of next-generation catalysts and corrosion inhibitors necessary to make the military more environmentally friendly and to prevent corrosion, thereby extending the lifetime of planes and ships.

2. Methodology

In order to treat complex physical and chemical processes accurately, first-principles methods are necessary. In traditional *ab initio* methods, this is done by explicitly expressing the many-electron wave function as a function of all electronic coordinates. By contrast, DFT treats the electronic charge density $n(\vec{r})$ as the basic variable of any system, and this allows the expression of the correlation effects as an effective potential acting on a set of one-particle wavefunctions. Because of the tremendous simplification of the electronic structure problem, DFT methods are much faster than wavefunction-based methods and have become the method of choice for the study of large systems.

It is well known that the core electrons are not involved in bonding and most other interesting physical and chemical behavior. The wavefunctions for the core electrons of an isolated atom will not be significantly different from those of the atom in a solid or molecule. Therefore, we can model the effect of the core electrons and the nucleus on the valence electrons by a pseudopotential. Because of the orthogonality requirement, the presence of the core states also requires the valence wavefunctions to oscillate in the core region. The presence of such sharp oscillations drastically increases the plane-wave cutoff of the calculations without providing any additional chemically relevant information. To eliminate the core electrons and to lower the plane-wave cutoff, we construct a pseudowavefunction which is identical to the all-electron wavefunction beyond the core cutoff radius r_c, but which is nodeless and smooth in the core region (for $r < r_c$). To ensure that the pseudo-wavefunctions accurately mimic the all-electron wavefunctions, the construction procedure enforces the preservation of the electronic scattering properties of the all-electron atom[3]. The reduction in the plane-wave cutoff and the elimination of the core electrons dramatically reduce the computational cost.

For all the DFT calculations presented here we use a plane-wave basis set. Such a basis set is complete and offers the advantage of carrying out operations in both real space and reciprocal space through the use of fast Fourier transforms. Calculations are done using the standard LDA[4] or GGA[5] exchange-correlation functionals using our in-house plane wave code and the DACAPO package. To reduce the computational cost of the calculations we use designed non-local[6] optimized[7] or ultra-soft[8] pseudopotentials to represent the interactions of the nucleus and the core electrons with the valence electrons. Minimization of the energy with respect to the electronic degrees of freedom is done using the blocked-Davidson[9] iterative diagonalization procedure[10] with Pulay density mixing[11]. Ionic minimization is performed using a quasi-Newton algorithm[12].

3. Results

In our research on piezoelectric oxides, we seek to understand the microscopic origin of the favorable properties of the current materials. We then apply our understanding to propose new alloys with improved properties. Temperature dependent effects are of crucial importance, and we therefore seek to create computational techniques that will allow us to model finite-temperature processes. In this paper, we present the results of our investigations into the local structure and phase transitions of the $Pb(Z, T_i)O_3$solid solution, development of a computationally inexpensive semi-empirical bond-valence model, and computational materials design studies of silver and lithium-based solid solutions for use in piezoelectrics. To understand the interactions of molecules and metal surfaces, we examine defects, chemisorption bonds, and adsorbate-adsorbate interactions that lead to the formation of ordered structures. In particular, we study metal vacancies, self-assembled monolayers on metal surfaces and the effect of strain on the interactions of CO with metal surfaces.

3.1. Local structure and phase transitions in $Pb(Z_r,T_i)O_3$.

Lead zirconate titanate (PZT) is currently the primary material used in naval SONAR devices. It is an alloy of two well-studied oxides, lead titanate[13] (PT) and lead zirconate(PZ)[14–16]. Like PT and PZ, PZT ($PbZr_{1-x}Ti_xO_3$) is a perovksite with the general formula, ABO_3. In the perovskite structure, the A cations (Pb) are in the

corners of the unit cell, the B cations (Zr/Ti) are in the center and the O anions are on each of the six faces of the cell.

On their own, neither PT nor PZ exhibit any favorable electrical properties. PT is a ferroelectric (FE) material with a simple tetragonal structure, while PZ has a complex antiferroelectric (AFE) ground state. It is the mixing of these materials which gives rise to high piezoelectricity. Within the ordered framework of the perovskite lattice, PZT has extensive disorder with respect to the distribution of B-cations into unit cells. Furthermore, there is disorder arising from the displacement of all of the ions from their high symmetry positions. This can be seen from the broadened peaks in the experimentally determined PZT pair distribution functions (PDF)[15] (Figure 1).

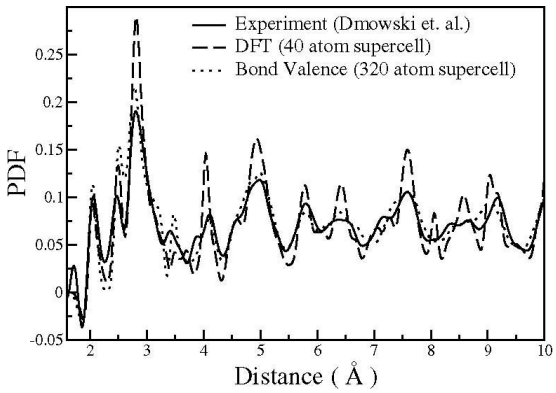

Figure 1. PDFs for 50/50 monoclinic PZT. Data are from experiment[15], DFT, and the BV model. Similar agreement with experiment was obtained with the BV model for the tetragonal and rhombohedral phases of PZT.

There are six phases in the composition/temperature phase diagram of PZT: a low temperature antiferroelectric phase, two rhombohedral phases at different temperatures (FE), a tetragonal phase (FE), a paraelectric high-temperature cubic phase, and the recently discovered low-temperature monoclinic (FE) phase around the 50/50 Zr/Ti composition[17]. The monoclinic phase is located at the morphotropic phase boundary between the tetragonal and the rhombohedral phases.

Recently, we used DFT calculations to elucidate the relationship between the microscopic local structure and the macroscopic phase transitions of the material[18]. In our DFT calculations, we see that all three cations distort significantly from their high-symmetry positions; however, the Pb motions are by far largest and determine the overall polarization of the material. We find that Pb ions move 0.4–0.5 Å, in perfect agreement with experimental results[14]. Pb atoms move mostly in tetragonal and monoclinic (orthorhombic) directions, even in the rhombohedral phase. The distortions are toward Ti neighbors and away from Zr neighbors, conforming to overall polarization as much as possible. Both preferences are understandable. Zr is a larger ion than Ti, which means that the purely repulsive interaction between Pb and B cations will be stronger for Pb-Zr than for Pb-Ti. Zirconium's larger size and smaller mobility inside the oxygen cage[15] also make it less able to accommodate the 0.4–0.5 Å Pb move. The repulsive interaction between Pb and the B-cations explains why (111) Pb distortions are rare. A large Pb displacement directly toward a B-cation incurs a large repulsive energy cost; therefore (100), (211), or (110) Pb distortions are preferred to the rhombohedral ones.

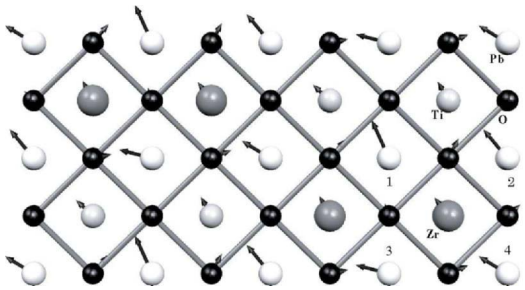

Figure 2. Projection of the 4 x 2 x 1 50/50 supercell DFT PZT structure onto the x–y plane. The oxygen octahedra are depicted by diamonds, and the distortions from the ideal cubic perovskite positions are shown by arrows. Pb atoms are 1/2 unit cell above the plane, and apical O atoms are omitted.

The conformity to overall direction of polarization is due to simple electrostatics which make dipole alignment favorable. In the case of Pb atoms 1 and 2 in Figure 2, both driving forces can be satisfied. However, in the case of Pb atoms 3 and 4, the local preference to move toward Ti conflicts with the desire to align with overall polarization. This competition results in a compromise, with distortions predominantly along the x-direction for these Pb atoms.

The interplay of the electrostatic dipole interactions and local A-B cation repulsion gives rise to compositional phase transitions. This is due to the strong dependence of the relative amounts of Zr-rich, neutral, and Ti-rich faces on Zr/Ti composition, as shown in Figure 3. At very low Ti content, most of the Pb atoms are located in all-Zr local environments. In such environments, ferroelectric Pb distortions are unfavorable as they would incur a large local repulsion energy cost. Instead, short Pb-O bonds are formed through a combination of small distortions and large octahedral rotations which bring O atoms close to Pb[14, 16]. A rotation of one octahedron creates a rotation of the neighboring octahedron in the opposite direction; this doubles the unit cell, resulting in antiferroelectricity. Thus, in an AFE phase, the

preference for dipole alignment is completely frustrated by the need to avoid the large local repulsion.

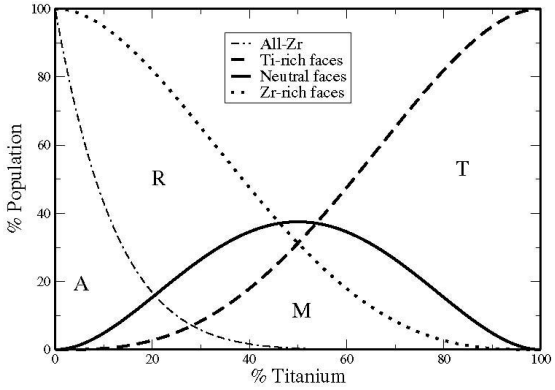

Figure 3. Populations of various Pb environments in PZT as a function of Ti composition. A, R, M, T denote the locations of the antiferoelectric, rhombohedral, monoclinic, and tetragonal PZT phases at low temperature.

The percentage of all-Zr environments declines rapidly as Ti content is increased. This decreases the local repulsion energy of a disordered ferroelectric rhombohedral phase, leading to an AFE-FE compositional phase transition on the Zr-rich side of the phase diagram. Since Zr-rich environments dominate, Pb atoms distort in a variety of directions that would give a longer Pb-Zr distance. This results in a large scatter in the directions of cationic displacements around the (111) axis. Thus, in the rhombohedral phase a compromise is reached between the dipole-dipole interactions and the local Pb-B repulsion interaction.

Near the 50/50 composition, the replacement of Zr-rich faces with neutral and Ti-rich faces allows some of the Pb distortions to rotate toward the (100) direction. Since approximately 30% of the Pb atoms are located in environments unfavorable to tetragonal distortion, this polarization rotation leads to a monoclinic phase, not a tetragonal one. On the Ti-rich side of the phase diagram, the (100) distortion satisfies the local energy and the dipole alignment preferences of most Pb atoms. Therefore a tetragonal phase is preferred.

Phase diagrams of perovskite solid solutions made by mixing an antiferroelectric such as PZ with PT, or a relaxor[19] ferroelectric such as PMN with PT, exhibit the same sequence of phase transitions with increasing Ti content; from parent antiferroelectric or relaxor ferroelectric, to a rhombohedral FE, to monoclinic FE, to a tetragonal FE phase.[20–22] This pattern can be explained in the framework of competition of dipole alignment and local repulsive interactions. In an antiferroelectric or relaxor material, an ordered ferroelectric distortion pattern would incur a large cost in local repulsion. As the smaller and more ferroelectric Ti cation is added, the A-B repulsive interactions become weaker and the local energy cost of ordered ferroelectricity is diminished. The material then undergoes a series of phase transitions: first to the disordered rhombohedral FE phase and then to a monoclinic FE phase and then to an ordered tetragonal FE phase.

3.2. Bond Valence Model – Efficiently Modeling Complex Oxides.

While DFT techniques have been proven to be effective in determining the local structural properties of complex oxide materials, DFT calculations have limitations. Due to the computational demands of DFT, it is not possible to use DFT to model very large supercells. This inhibits the ability to use DFT to study mesoscopic phenomena such as domain wall shifting, ion transport, and doping and vacancy effects which are particularly important for the next-generation relaxor-based piezoelectrics such PMN-PT and PZN-PT. In addition, DFT is a zerotemperature probe, making it difficult to extract finite-temperature properties from *ab initio* calculations.

Extensive research has been performed to develop DFT-based semi-empirical and phenomenological models for studying finite temperature properties of large ferroelectric systems[23–27]. It has been shown that such methods can be used to perform molecular dynamics and Monte Carlo simulations to predict temperaturedependent phase transitions in oxides and to calculate phonon mode spectra. However, to date these methods have been hampered by the omission of high-energy degrees of freedom which lead to inaccuracies in simulation, as well as by the difficulty of by-hand parameterization.

To successfully study complex piezoelectrics, the proposed model must account for compositional differences in a single system and be transferable from one system to another. Our model is based on the bond-valence theory[28], a well-known concept in crystal chemistry, which has been used to assess the validity of various chemical structures. Recently, other theorists have also begun to employ bond-valence based methods[29]. The bond-valence theory relates the bond strength (or valence) of an ionic pair to the inter-atomic distance. When the ions are sufficiently separated, there is no bonding interaction between them. As they move closer to each other there is an inverse power relation between the bond strength and the bond distance (Equation 1).

$$s_{ij} = \left(\frac{R_{ij}}{R_0} \right)^{N_{ij}} \quad (1)$$

Here R_{ij} is the distance between the two ions, R_0 is the length of a bond that would give a valence of 1, and N determines the rate of decay of the bonding interaction between the ith and j th ions. In a crystal structure, each ion will make bonding interactions such that the sum of all its bond-valences is equal to its nominal valence.
Bond-valence arguments can correctly predict which crystal structures are favored. However, we find that this concept alone cannot model structural distortions in complex ionic crystals. Therefore, we proceed to construct a potential which reflects each atom's desire to fulfill its bond valence. From this, we define an energy due to the bond-valence interactions:

$$E_{\mathrm{BV}} = \sum_i A_i \left[\left| V_i V_i^0 \right|^{\alpha_i} (V_i^0)^{\alpha_i} \right], \qquad (2)$$

Here V_i is the actual valence of the ith ion and V_i^0 is the nominal valence of that ion. A_i and α_i affect the total energy and the forces of the ion and are necessary for matching the BV forces and energies to DFT forces and energies. Figure 4 shows the form of the bond valence potential.

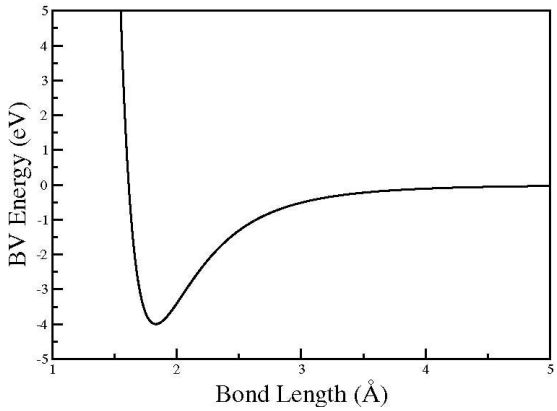

Figure 4. This plot shows the bond-valence energy dependence on distance for a diatomic molecule, as defined in our bond-valence model. The bond-valence concept has been modified to assign an energy cost to each atom's inability to obtain its desired valence.

One shortcoming of the bond-valence theory is that it does not include long-range electrostatic interactions, which play an important role in ionic systems such as the ferroelectric perovskites. To account for this, we use an Ewald summation (E_{ewald}) to calculate the long range Coulombic interactions. An additional short-range repulsive term (E_{rep}) is included (Equation 3) to prevent unphysically short distances which arise when only the Ewald and BV terms are used.

$$E_{rep} = \sum_{ij} A_{ij} e^{-B_{ij} R_{ij}} \qquad (3)$$

A first generation of our model was parameterized by hand and was able to correctly predict the distortion patterns of small regions of 50/50 monoclinic PZT (Figure 5) found by our DFT calculations (Figure 2) and was then used to reproduce experimental pair distribution function (PDF) of PZT solid solution.

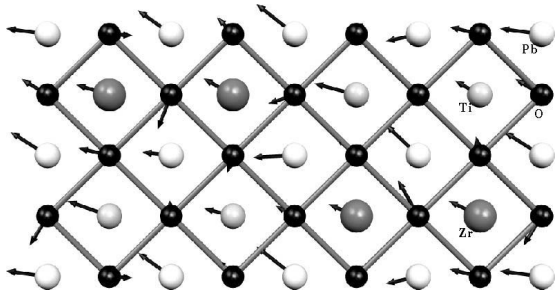

Figure 5. Bond-valence model distortion pattern for same structure shown in Figure 2.

Figure 1 depicts the experimental PDF for the 50/50 monoclinic phase of PZT[15] and the PDFs calculated from relaxed 40-atom DFT and 320-atom BV model 50/50 monoclinic supercell structures. The experimental results were obtained at 10 K, thus limiting the effects of thermal motion within the material. The widths of the peaks in the experimental PDF show the extensive structural disorder. The narrow peaks of the DFT PDF show that the DFT supercell is too small and ordered to fully reproduce the experimental PDF. The BV model has the advantage of being able to model larger, more disordered supercells, correctly reproducing the experimental PDF with a 320-atom supercell. Similar agreement was observed for both the 40/60 tetragonal and 60/40rhombohedral phases. This points to the transferability of the BV model. The model also correctly predicted phase transition from 60/40 rhombohedral to 50/50 monoclinic to 40/60 tetragonal phases, demonstrating that B-cation disorder combined with intuitive inter-atomic interactions is sufficient to reproduce and explain the complicated behavior of PZT as seen by disordered PDFs and compositional phase transitions.

A second generation of the model was then parameterized to reproduce the DFT forces and cohesive energies of twenty different structures, in order to extend the use of the model to finite-temperature molecular dynamics simulations. To automate the parameterization we used a simulated annealing procedure, obtaining model parameters that give the best agreement between BV and DFT forces and energy differences. An average force deviation of 0.03 eV/Å for a single coordinate and

cohesive energy deviation of 0.005 eV per atom were obtained. A comparison of DFT and BV forces for a sample structure is presented in Table 1 and Figure 6. The excellent agreement between the BV and DFT results is very promising for the use of this model in realistic modeling of mesoscopic processes in piezoelectrics.

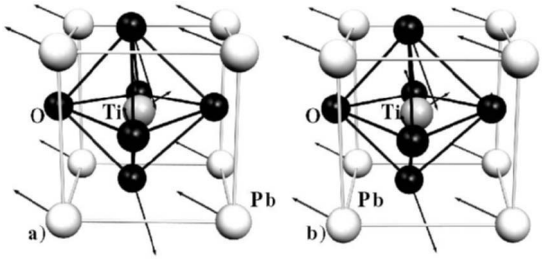

Figure 6. Optimized BV parameters are able to accurately reproduce DFT (a) forces (portrayed as arrows) on a high-energy test structure. The parameters obtained from the BV optimization routine give BV forces (b) that agree with DFT forces within an average deviation of 0.032 eV/Å per coordinate.

Table 1. DFT and optimized bond-valence forces on atoms for a high-energy structure of $PbTiO_3$.

Species	*x* (eV/Å)	*y* (eV/Å)	*z* (eV/Å)
Pb(DFT)	-0.97	0.25	-0.59
Pb(BV	-0.97	0.32	-0.58
Ti(DFT)	0.59	0.29	-0.38
Ti(BV)	0.57	0.28	-0.39
O_1 (DFT)	-0.17	0.74	0.93
O_1 (BV)	-0.11	0.73	0.88
O_2 (DFT)	0.54	-1.49	0.22
O_2 (BV)	0.48	-1.54	0.27
O_3 (DFT)	0.01	0.21	-0.18
O_3 (BV)	-0.02	0.17	-0.19

3.3. DFT study of silver piezoelectrics.

The superior performance of PZT that made it the mainstay of piezoelectric devices is due to the off-centering behavior exhibited by Pb atoms on the perovskite A-site as well as the presence of the morphotropic phase boundary (MPB) in the PZT phase diagram. Large cation off-centering gives rise to a large dipole moment and strong coupling to electric fields; this is there- fore crucial for high piezoelectric performance. However, due to the toxicity of Pb, more environmentally-friendly materials are actively being sought as possible replacements for PZT. To preserve the large internal polariza- tion of Pb-based oxides, the proposed lead-free solid solutions must display similar off-centering behavior. However, of the cations known to occupy the perovskite A- site at ambient pressure and temperature, only four have been shown to exhibit off-centering behavior: Pb, Cd, Bi, and Li. Unfortunately, Bi[30] and Cd are both toxic, and therefore are not good candidates for environmentally- friendly piezoelectrics. Lithium is not toxic and displays a very large off-centering of 1.0 Å[31], but its small size gives rise to limited solubility in the perovskite phase, as described in the next section.

Extending our computational methodology to materials design, we therefore investigated the properties of ferroelectric solid solutions containing Ag atoms on the perovskite A-site. Since Ag is a neighbor of Cd in the periodic table, we propose that it may display similar behavior. Since Ag is non-toxic, Ag off-centering may open the possibility of truly environmentally-friendly high performance piezoelectrics.

The most widely studied perovskite with Ag on the A-site is $AgNbO_3$[32–34]. $AgNbO_3$ can be easily made using conventional solid-state synthesis methods. Dielectric properties of $AgNbO_3$ and solutions of $AgNbO_3$ with $AgTaO_3$ as well as Li, Na, and K substitutions were recently studied[32]. $AgNbO_3$ assumes six structural phases with increasing temperature. At low temperature it is found in either a weak ferroelectric or ferrielectric orthorhombic phase; at 340 K it undergoes a transition to an antiferroelectric phase, a second antiferroelectric phase appears at 540 K and at 626 K $AgNbO_3$ becomes paraelectric. Two more paralectric phases appear at higher temperatures. The lattice parameters of the low-temperature phase have been determined by X-ray diffraction to be a=3.91 Å and c=3.94 Å.

We have found that Ag atoms demonstrated large off- centering behavior in solid solutions with $PbTiO_3$ (PT) and PZT. We first study $AgNbO_3$ in a 5-atom unit cell. We find that at the experimental volume, both silver and niobium off-center significantly; silver distorts by 0.5 Å, similar to the Pb off-centering in $PbTiO_3$ and to the Cd off-centering in $(Pb,Cd)TiO_3$. In $PbTiO_3$, Pb atoms distort along the (100) direction, splitting Pb-O bonds into three equal groups of four short (2.4–2.5 Å), medium (2.7–2.9 Å) and long (3.1–